Sensors and Materials, Vol. 36, No. 9 (2024) 3787–3796
MYU Tokyo

S & M 3767

Dissipation Energy as a Method for Sensing the Tribology Mechanism

Shih-Chen Shi,[1*] Tao-Hsing Chen,[2] Chih-Chia Wang,[3,4]
Hao-Fu Zhang,[1] Yue-Feng Lin,[5] and Dieter Rahmadiawan[1,6]

[1]Department of Mechanical Engineering, National Cheng Kung University, Tainan 70101, Taiwan
[2]Department of Mechanical Engineering, National Kaohsiung University of Science and Technology, Kaohsiung 80778, Taiwan
[3]Department of Chemical and Materials Engineering, Chung Cheng Institute of Technology, National Defense University, Taoyuan 335009, Taiwan
[4]System Engineering and Technology Program, National Yang Ming Chiao Tung University, Hsinchu 300093, Taiwan
[5]Department of Mechanical Engineering, National Chin-Yi University of Technology, Taichung 411030, Taiwan
[6]Department of Mechanical Engineering, Universitas Negeri Padang, 25173 Padang, Sumatera Barat, Indonesia

(Received April 18, 2024; accepted June 24, 2024)

Keywords: cellulose nanofiber, composite, wear, mechanism, sensor

In this study, we demonstrated that adding 0.05 wt.% cellulose nanofibers (CNFs) to CNF-poly(methyl methacrylate) (PMMA) composite materials enhanced hardness, toughness, and maximum flexural strength, surpassing commercially available PMMA variants. Furthermore, CNF addition substantially improved PMMA's wear resistance, reducing wear volume through increased hardness and CNF's lubricating effect. The observed variation in slope in the wear volume versus dissipated energy plot suggests different wear mechanisms, and the potential to serve as a sensor for detecting wear interface behavior.

1. Introduction

The utilization of products derived from natural materials is increasingly prevalent across various application domains, each with unique material requirements.[1,2] A common approach to address these diverse demands involves modifying materials by incorporating fillers.[3] The nanostructure of these fillers has emerged as a prominent area of investigation in recent years.

Under conditions of optimal dispersion, nanosized fillers exhibit pronounced nanoscale effects and generate a substantial interfacial area within the matrix.[4] The properties of this interface significantly affect the overall characteristics of the composite material. Nanocellulose, distinguished by its exceptional mechanical properties, biodegradability, and renewability, has attracted significant research interest in nanocomposite materials.[5]

Tribology is a discipline in which the phenomena and principles of friction, wear, and lubrication occurring between two contacting bodies in relative motion are investigated.[6,7] With current considerations for Sustainable Development Goals (SDGs) and Earth sustainability,

*Corresponding author: e-mail: scshi@mail.ncku.edu.tw
https://doi.org/10.18494/SAM5080

ISSN 0914-4935

green tribology, characterized by non-biotoxicity and minimal environmental and ecosystem impact, has garnered increased attention.[8] The three core concepts of green tribology are (1) the utilization of environmentally and human-friendly green materials,[9] (2) the minimization of pollutants and harmful substances emitted during the design, manufacturing, and usage of products,[10] and (3) the maximization of lubrication reaction and efficiency.[11] Designing appropriate tribological mechanisms for specific applications to maximize lubrication efficiency has become increasingly crucial.[12,13]

The study of cellulose nanofiber (CNF) can be traced back to 1983 when Herrick *et al.*[14] and Turbak *et al.*[15] utilized repeated high-pressure homogenization to fibrillate cellulose through rapid shear action. Subsequently, various mechanical methods have been developed, including high-intensity ultrasonication,[16] grinding,[15] cryo-crushing,[17] twin-screw extrusion,[18] steam explosion,[19] ball milling,[20] and water jet cutting.[21] Among these, the mainstream methods are high-pressure homogenization and grinding.

In this study, we used CNF extracted from purified straw and biocompatible poly(methyl methacrylate) (PMMA) to fabricate a CNF-PMMA composite material system. We posited that CNF filler would be displaced from the PMMA composite during wear, forming a novel tribolayer on the surface. This tribolayer was expected to furnish a friction interface lubrication mechanism. By examining the wear characteristics of CNF nanoadditives in biopolymer composites, the alterations in friction mechanisms attributable to CNF tribolayers can be elucidated.

2. Materials and Methods

2.1 Preparation of CNF

The CNF processing involved three main steps: pretreatment, pulping, and CNF extraction. Pretreatment entailed the refinement of straw using a grinder. Pulping consisted of the removal of impurities such as lignin and hemicellulose from the straw through an alkaline process and bleaching to obtain pure cellulose material.[22] CNF extraction included adding 0.016 g of TEMPO and 0.01 g of sodium bromide to 100 mL of deionized water, followed by sonication for 1 min. Subsequently, 1 g of purified cellulose was placed in a beaker, sodium hypochlorite was added, and the pH was maintained at 10 using a 0.05 M sodium hydroxide solution. After the reaction, vacuum filtration was performed, and the residue was rinsed with deionized water.

2.2 Preparation of CNF/PMMA composite materials

In a controlled laboratory setting, 270 mL of methyl methacrylate (MMA) monomer was meticulously measured and combined with 0.0333 wt.% benzoyl peroxide (BPO) initiator within a designated prepolymerization vessel. Subsequently, the amalgamation underwent a gentle agitation to ensure homogeneous distribution and thorough blending of the constituents. The prepolymerization bottle was placed in a thermostatic water bath at 88 °C for 20 min. After the prepolymerization, the bottle was cooled to 25 ℃ for 15 min. Upon reaching room temperature,

varying amounts of CNF were added, and intermittent sonication was performed using a 720 W ultrasonic cell disruptor to disperse the nanoscale powder within the monomer uniformly. After mixing, the prepolymerization bottle was returned to the thermostatic water bath at 88 °C for 25 min of polymerization. The mixture was then poured into molds and placed in a thermostatic water bath at 68 °C for 3 h. After removal from the molds, the specimens were transferred to a 90 °C oven and baked for 1 h.

2.3 Characterization of CNF/PMMA composites: mechanical and tribological properties

The tensile properties of the composite materials were assessed in accordance with the standard specifications outlined in ASTM D638. Flexural properties were tested following ASTM D790 standards. Tribological characteristics were evaluated by rotary wear testing and the observation of wear tracks using a 3D laser scanning microscope.

3. Results and Discussion

3.1 Mechanical properties of CNF/PMMA composite materials

Upon the addition of CNF, the hardness of the PMMA composite materials increased significantly, as depicted in Fig. 1. This phenomenon indicates that after the addition of CNF, the actual contact area of PMMA under the same load is smaller, resulting in a noticeable enhancement in load-bearing capacity.

The tensile strength of pure PMMA was 67.86 ± 2.97 MPa, with a fracture strain of only 4.13%. Upon adding 0.05 wt.% CNF, the tensile strength increased to 73 MPa, accompanied by increased fracture strain and toughness, as shown in Fig. 2. At 0.1 wt.%, there was a slight decrease in both tensile strength and fracture strain. Beyond 0.5 wt.%, both tensile strength and toughness exhibited significant reductions. Agglomeration was observed in composite materials

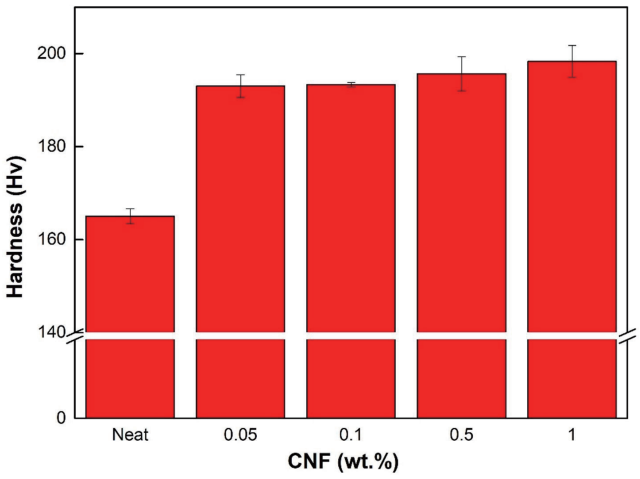

Fig. 1. (Color online) Hardness test results of composite materials.

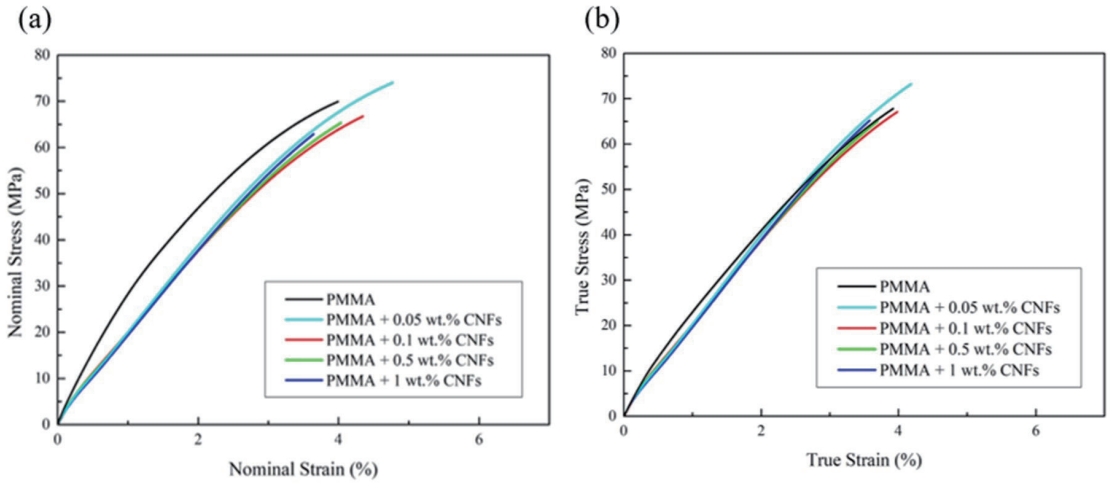

Fig. 2. (Color online) (a) Engineering stress–strain curves and (b) true stress–strain curves of CNF-PMMA composites.

with CNF additions of 0.1 wt.% and above, with the number of agglomerates increasing with the amount of addition, leading to stress concentration and subsequent reductions in tensile strength and toughness. No significant agglomeration was observed at 0.05 wt.%.

The flexural strength and flexural modulus of the CNF-PMMA composites showed slightly enhanced behavior with the addition of 0.05 wt.% CNF. However, for composite materials with CNF additions exceeding 0.1 wt.%, flexural strength and modulus decreased, consistent with the trend observed in the tensile strength results, as shown in Fig. 3. This trend is presumed to be due to the mechanism causing the strengthening effect. Despite the decrease in flexural strength and modulus with excessive CNF addition, they remained significantly higher than the original properties of PMMA, which had a bending strength of 65 MPa and a modulus of 2 GPa, and were also higher than that of commercially available injection-molded and compression-molded PMMA.

3.2 Tribological behavior of CNF/PMMA composites

A physiological saline solution was used as a lubricant during wet abrasion. The wear volume and average coefficient of friction during dry abrasion were larger than those during wet abrasion. Both dry and wet abrasions exhibited similar trends. Upon the incorporation of CNF, there was a notable decrease in wear volume and friction coefficient, with the antiwear effect increasing with the augmentation of additive quantity, as illustrated in Fig. 4. The CNF-PMMA composite materials demonstrated superior wear resistance in dry and wet environments.

To elucidate the role of CNF in the wear process, wear experiments were conducted at three different distances, as illustrated in Fig. 5. Despite increasing abrasion distance, the CNF-PMMA composite material maintained superior wear resistance. As PMMA undergoes abrasion, surface abrasion marks are initially formed, resulting in the most extended abrasion length

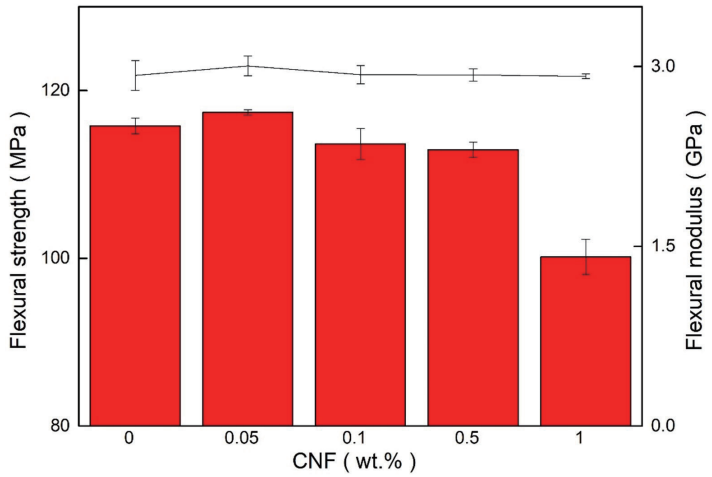

Fig. 3. (Color online) Bending test results of CNF-PMMA composites.

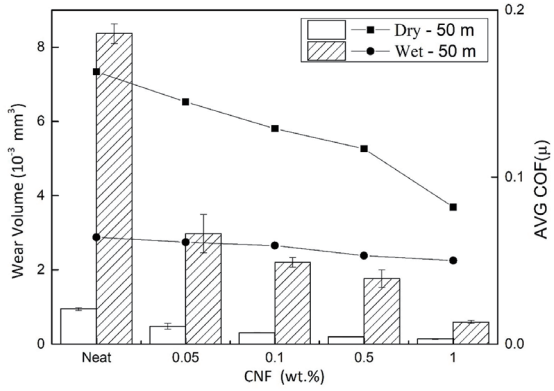

Fig. 4. Wear volume and average friction coefficient of composites (dry/wet test, wear distance 50 m).

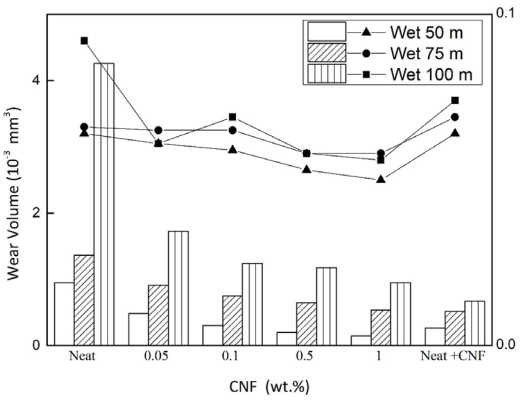

Fig. 5. Wear volume and average friction coefficient of the composites (wet test, wear distances 50/75/100 m).

occuring within the wear distance range of 0 to 50 m, yet exhibiting the least wear volume among the three segments.

Wear volumes for each segment were calculated to examine the wear characteristics of PMMA, as depicted in Fig. 6. The wear volume is lower in the 0–50 m range, whereas a significant increase is observed in the 75–100 m range. Compared with pure PMMA, within the initial 50 m and the 75–100 m range, the wear volume is lower for the composite materials. Owing to the higher surface hardness of PMMA, most of the wear in the 0–50 m interval is attributed to surface abrasion, resulting in a lower wear volume. However, after the formation of abrasion marks, the wear volume of PMMA substantially increases owing to the increase in the actual contact area. The addition of CNF enhances the surface hardness of the composite material, indicating an improvement in load resistance. In the initial wear stage, it is more

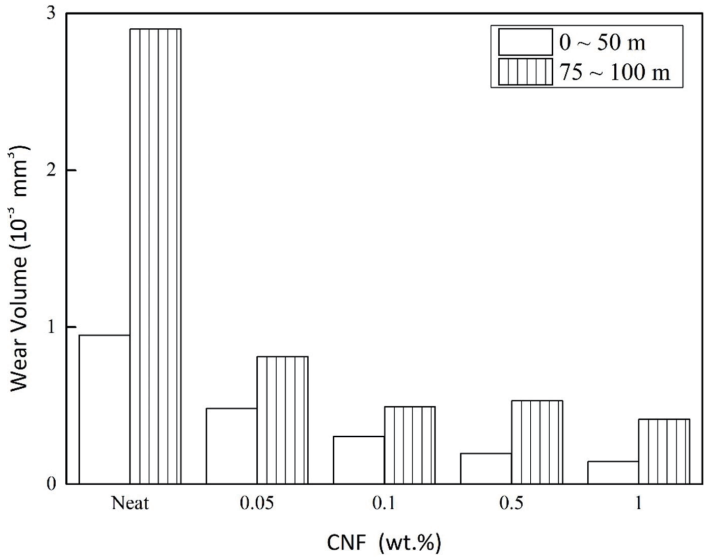

Fig. 6. Wear volumes within various distance intervals for the composites.

challenging to produce abrasion marks, thus reducing the wear volume in the 0–50 m range for CNF-added PMMA.

Additionally, the wear volume of the CNF-added PMMA is lower than that of pure PMMA in the 75–100 m range, suggesting a specific lubricating effect of CNF during the wear process. A physiological saline solution mixed with CNF was added as a lubricant during the abrasion of pure PMMA to test the lubricating effect of CNF, as depicted in Fig. 5. The addition of CNF resulted in a significant decrease in wear volume, approaching the wear test result of the 1 wt.% composite material. As discussed in Sect. 4.3.2, the lower surface hardness of pure PMMA leads to higher wear volume at 50 m, while at 75 and 100 m, the wear volume decreases owing to the presence of CNF, demonstrating the lubricating effect of CNF.

Figures 7 to 10 show that at an abrasion distance of only 50 m, the surface of pure PMMA already began to exhibit abrasion marks. In contrast, the composite materials with added CNF only showed minor traces on the surface, and even the 1 wt.% CNF composite exhibited only some scratches. As the abrasion distance increased to 75 m, the abrasion marks became increasingly noticeable, and by 100 m, significant abrasion marks were evident.

3.3 Wear mechanism and sensing behavior

The relationship between wear volume and dissipated energy is shown in Fig. 11. It can be seen that as the concentration of CNF increases, there is a noticeable decrease in wear volume for the same dissipated energy. Specifically, the sample with 1% CNF shows a significantly lower wear volume at higher energy levels, illustrating the reinforcing effect of the nanofibers. This can be attributed to the enhanced interfacial adhesion between the PMMA matrix and the CNF, which improves the load transfer capabilities and thus reduces the material loss due to wear.[23]

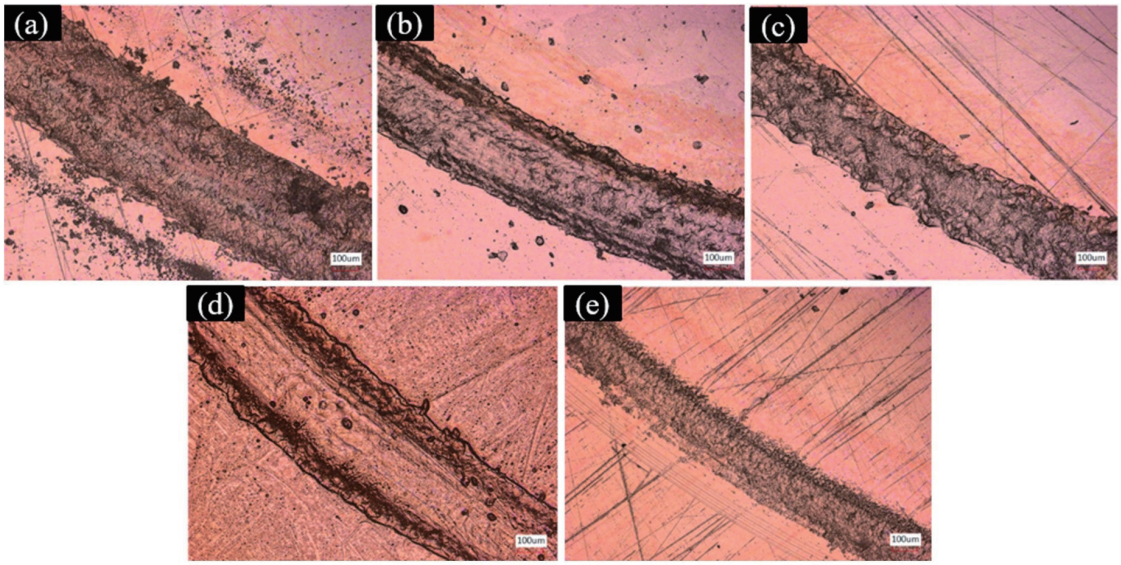

Fig. 7. (Color online) 3D laser scanning images of dry wear at 50 m for the composites: (a) neat, (b) 0.05 wt.%, (c) 0.1 wt.%, (d) 0.5 wt.%, and (e) 1 wt.%.

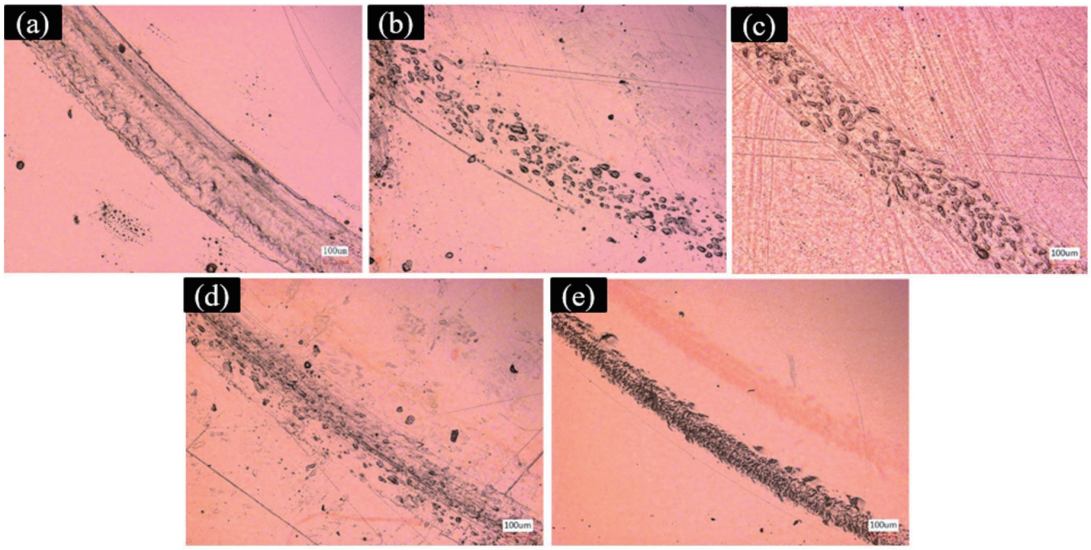

Fig. 8. (Color online) 3D laser scanning images of wet test at 50 m for the composites: (a) neat, (b) 0.05 wt.%, (c) 0.1 wt.%, (d) 0.5 wt.%, and (e) 1 wt.%.

The linear fit lines for each composite concentration suggest that the wear mechanism remains consistent across different energy levels, which validates the use of a single wear coefficient in accordance with Archard's Law for each composite composition. However, the slope of these lines varies with the CNF content, indicating a change in wear resistance. The sample with the highest CNF content has the lowest slope, which implies a reduced wear rate. It is also worth noting that the slope of the wear volume versus energy curve provides an estimate

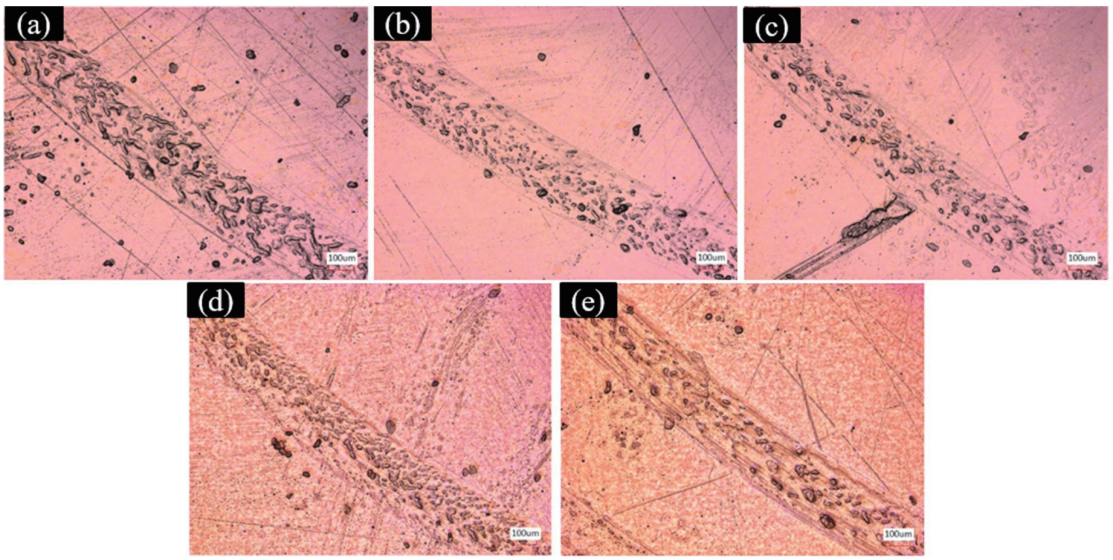

Fig. 9. (Color online) 3D laser scanning images of wet test at 75 m for the composites: (a) neat, (b) 0.05 wt.%, (c) 0.1 wt.%, (d) 0.5 wt.%, and (e) 1 wt.%.

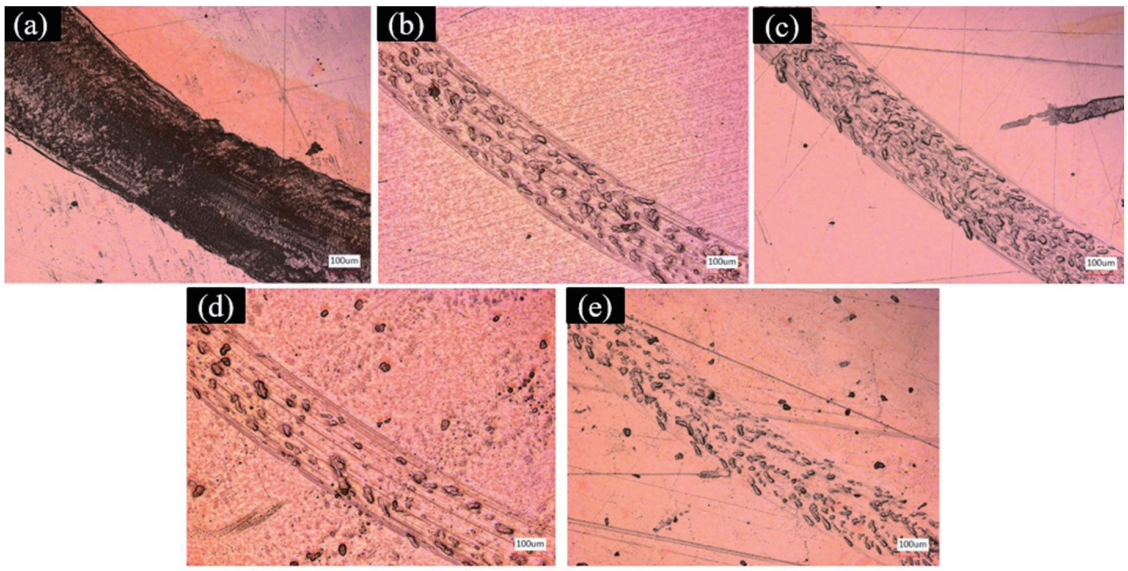

Fig. 10. (Color online) 3D laser scanning images of wet test at 100 m for the composites: (a) neat, (b) 0.05 wt.%, (c) 0.1 wt.%, (d) 0.5 wt.%, and (e) 1 wt.%.

of the wear coefficient of Archard's Law.[24,25] The decreasing slope with increasing CNF content may indicate an increase in the effective hardness of the composite, which is consistent with the hardness value achieved in Fig. 1.

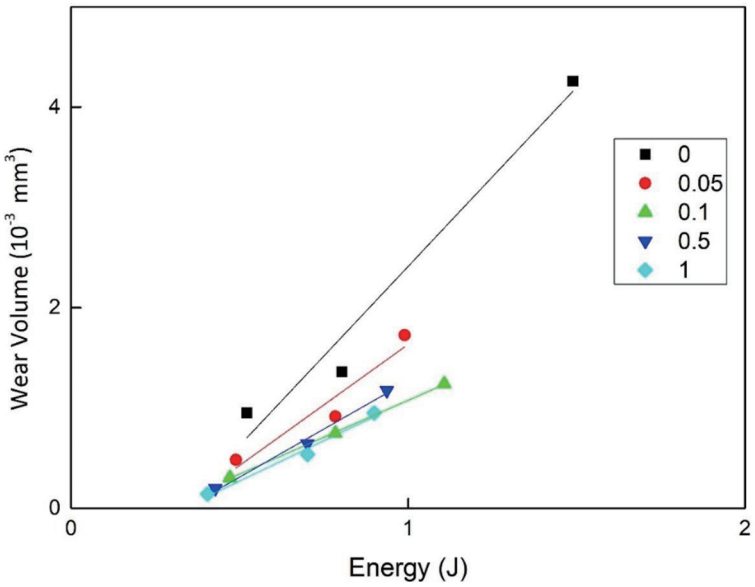

Fig. 11. (Color online) Relationship between wear volume and dissipated energy for the composites.

4. Conclusions

In the study of the mechanical properties of CNF-PMMA composite materials, the addition of 0.05 wt.% CNF successfully enhanced hardness, toughness, and maximum flexural strength, suggesting the reinforcement effect of the composite materials. Moreover, the flexural strength exceeded those of commercially available injection-molded and compression-molded PMMA. Regarding the wear properties of CNF-PMMA composite materials, it was found that the addition of CNF significantly improved the wear properties of PMMA, with a considerable reduction in wear volume during the wear process, as a result of the increased hardness and the lubricating effect of CNF. Finally, the variation in slope observed in the relationship between wear volume and dissipated energy for the composite materials can indicate different wear mechanisms. This phenomenon can be utilized as a sensor for sensing wear interface behavior.

Acknowledgments

This work was supported by the National Science and Technology Council, Taiwan (grant number 112-2221-E-006-173, 113-2221-E-006-087-MY2, 113-2221-E-006-112-MY2, and 113-2221-E-006-116). The authors gratefully acknowledge using EM000700 equipment belonging to the Core Facility Center of National Cheng Kung University. The authors gratefully acknowledge the Core Facility Center of National Cheng Kung University. This research was partly supported by the Higher Education Sprout Project, Ministry of Education to the Headquarters of University Advancement at National Cheng Kung University (NCKU).

References

1 H. Nurdin, W. Waskito, A. N. Fauza, B. M. Siregar, and B. K. Kenzhaliyev: Teknomekanik **6** (2023) 94. https://doi.org/10.24036/teknomekanik.v6i2.25972
2 A. N. Fauza, F. Qalbina, H. Nurdin, A. Ambiyar, and R. Refdinal: Teknomekanik **6** (2023) 21. https://doi.org/10.24036/teknomekanik.v6i1.21472
3 S.-C. Shi, X.-N. Tsai, and D. Rahmadiawan: Surf. Coat. Technol. **483** (2024) 130712. https://doi.org/10.1016/j.surfcoat.2024.130712
4 U. V. Akhil, N. Radhika, B. Saleh, S. Aravind Krishna, N. Noble, and L. Rajeshkumar: Polym. Compos. **44** (2023) 2598. http://dx.doi.org/https://doi.org/10.1002/pc.27274
5 D. Rahmadiawan, S.-C. Shi, H. Abral, M. K. Ilham, E. Sugiarti, A. N. Muslimin, R. A. Ilyas, R. Lapisa, and N. S. D. Putra: J. Nat. Fibers **21** (2024). https://doi.org/10.1080/15440478.2023.2301386
6 B. Bhushan: Principles and Applications of Tribology (John Wiley & Sons, 2013).
7 D. Rahmadiawan, S.-C. Shi, Z. Fuadi, H. Abral, N. Putra, R. Irwansyah, D. Gasni, and A. M. Fathoni: Jurnal Tribologi **39** (2023) 36.
8 S.-w. Zhang: Friction **1** (2013) 186. http://dx.doi.org/10.1007/s40544-013-0012-4
9 S.-C. Shi and T.-F. Huang: Surf. Coat. Technol. **350** (2018) 997. https://doi.org/10.1016/j.surfcoat.2018.03.039
10 S.-C. Shi, T.-H. Chen, and P. K. Mandal: Polymers **12** (2020) 1246. https://doi.org/10.3390/polym12061246
11 M. Nosonovsky and B. Bhushan: Green Tribology (Springer, 2012).
12 S.-C. Shi and J.-Y. Wu: Surf. Coat. Technol. **350** (2018) 1045. https://doi.org/10.1016/j.surfcoat.2018.02.067
13 D. Rahmadiawan, H. Abral, S.-C. Shi, T.-T. Huang, R. Zainul, A. Ambiyar, and H. Nurdin: Tribol. Ind. **45** (2023) 367. http://dx.doi.org/10.24874/ti.1482.05.23.06
14 F. W. Herrick, R. L. Casebier, J. K. Hamilton, and K. R. Sandberg: J. Appl. Polym. Sci.: Appl. Polym. Symp. (United States) **37** (1983).
15 A. F. Turbak, F. W. Snyder, and K. R. Sandberg: J. Appl. Polym. Sci.: Appl. Polym. Symp. (United States) **37** (1983).
16 W. Chen, H. Yu, Y. Liu, Y. Hai, M. Zhang, and P. Chen: Cellulose **18** (2011) 433. https://doi.org/10.1007/s10570-011-9497-z
17 A. Bhatnagar and M. Sain: J. Reinf. Plast. Compos. **24** (2005) 1259. https://doi.org/10.1177/0731684405049864
18 T. T. T. Ho, K. Abe, T. Zimmermann, and H. Yano: Cellulose **22** (2015) 421. https://doi.org/10.1007/s10570-014-0518-6
19 B. M. Cherian, A. L. Leão, S. F. de Souza, S. Thomas, L. A. Pothan, and M. Kottaisamy: Carbohydr. Polym. **81** (2010) 720. https://doi.org/10.1016/j.carbpol.2010.03.046
20 L. Zhang, T. Tsuzuki, and X. Wang: Cellulose **22** (2015) 1729. https://doi.org/10.1007/s10570-015-0582-6
21 R. Kose, I. Mitani, W. Kasai, and T. Kondo: Biomacromolecules **12** (2011) 716. https://doi.org/10.1021/bm1013469
22 S.-C. Shi and G.-T. Liu: Cellulose **28** (2021) 6147. http://doi.org/10.1007/s10570-021-03889-5
23 J. X. Chan, J. F. Wong, M. Petru, A. Hassan, U. Nirmal, N. Othman, and R. A. Ilyas: Polymers (Basel) **13** (2021) 2867. http://dx.doi.org/10.3390/polym13172867
24 C. Özorak and S. Islak: Mater. Chem. Phys. **314** (2024) 128903. https://doi.org/10.1016/j.matchemphys.2024.128903
25 D. Rahmadiawan and S.-C. Shi: Sci. Rep. **14** (2024) 9217. http://dx.doi.org/10.1038/s41598-024-59010-w